Melting curve analysis in a snapshot

Philipp Baaske, Stefan Duhr, and Dieter Braun[a)]
Department of Applied Physics, Ludwig-Maximilians-University, Amalienstrasse 54, 80799 Munich, Germany

The thermal denaturation of molecules is an essential method in biochemistry and diagnostics, including the measurement of single nucleotide polymorphisms and the binding analysis of proteins. We present a method for the all-optical high speed measurement of melting curves. A thin sheet of water is locally heated with an infrared laser to obtain a spatial temperature distribution between 20 and 100 °C. Using a fluorescence microscope a melting curve is recorded within 50 ms. This is about 10 000-times faster than state-of-the-art fluorometry and yields the same results for the validation example of a DNA hairpin. © *2007 American Institute of Physics.*
[DOI: 10.1063/1.2790806]

Measuring the stability of biomolecules and especially of DNA is of great importance in the field of biology, medical diagnostics, and biotechnology. It is often inferred from thermal denaturation experiments[1] and directly provides information about the DNA sequence or the biomolecular structure. In most cases, the conformation of the molecules is recorded by fluorescence and is plotted against temperature, yielding a so-called melting curve.[2] Traditionally, a small sample volume inside a comparably large cuvette or multiwell plate is heated by thermal contact. The thermal mass of the setup results in long equilibration times and slow heating rates. Measurement times on the order of 6–70 min are typical.[3]

We developed an all-optical method to determine the thermal stability of biomolecules in less than 50 ms. The temporal scan of temperatures is replaced by the application of a spatial temperature distribution, generated by heating a 20 μm thin fluid film with an infrared laser. The measurement volume is 2 nl and concentrations in the 100 nM regime are accessible due to sensitive fluorescence imaging with high numerical aperture optics. Typically, a fluorescence dye reports the conformation of molecules in a melting curve. In our case we measured a DNA hairpin which was labeled with a fluorophore quencher pair, a configuration termed molecular beacon.[4,5]

The melting of biomolecules is often approximated using a two state model, which requires information over a wide temperature range to reach the completely closed and completely open states. In our experiment, a spatial temperature distribution with all temperatures between ambient temperature and 100 °C was achieved with a temperature resolution <1 °C. Such high resolution melting curves can be used for single nucleotide polymorphisms detection, genetic screening, and biomolecule binding assays.[6–8]

We generate a broad spatial temperature distribution by focusing an infrared laser into a 20 μm thin sheet of aqueous solution. Temperatures between 20 and 100 °C are created within several milliseconds in a field of view of 200×200 μm^2. Imaging is provided with a fluorescence microscope with a 40$\times$ oil immersion objective and a charge coupled device (CCD) camera (Fig. 1).

The precise timing of events is necessary to prevent artifacts from thermophoresis. Initially, a fluorescence image $I_0(x,y)$ with 10 ms exposure time is taken at an ambient temperature. Then, the infrared laser is switched on within 1 ms. A second image $I_1(x,y)$ is taken after 40 ms. The images I_0 and I_1 are corrected against camera background and bleaching. Measuring the fluorescence ratio $R(x,y) = I_1(x,y)/I_0(x,y)$ ensures the removal of artifacts from an inhomogeneous illumination [Fig. 2(a)].

As described below, the temperature distribution is imaged using temperature dependent fluorescence. The resulting temperature image $T(x,y)$ is shown in Fig. 2(b). In principle, the ratio $R(x,y)$ could be plotted against the temperature $T(x,y)$ for each pixel. However, the initial radial averaging of both $R(x,y)$ to $R(r)$ and $T(x,y)$ to $T(r)$ with radius r improves the signal to noise ratio since the low signals toward the periphery are averaged over an increased number of pixels. The resulting melting curve $F(T) = [R(T) - R_{min}]/(R_{max} - R_{min})$ is plotted in Fig. 2(c) (circles). R_{min} is the fluorescence ratio of the completely closed state and R_{max} of the completely open state, respectively. The melting curve measured in only 50 ms agrees well with a 120 min lasting melting curve measured using a fluorometer [Fig. 2(c), solid line]. The slight shift between the curves most likely stems from temperature variations due to differences in the chamber thickness between the hairpin and the temperature measurement.
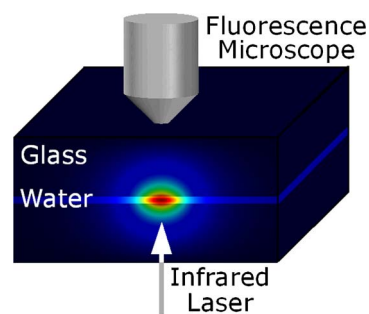

FIG. 1. Setup: Fluorescence from molecules in a 20 μm thin sheet of water is imaged from the top while it is heated with a focused infrared laser from below. Plotting the fluorescence image vs the temperature yields a high speed measurement of a melting curve at low molecule concentration. Color coded is the simulated temperature field.

a)Author to whom correspondence should be addressed. Electronic mail: dieter.braun@physik.lmu.de
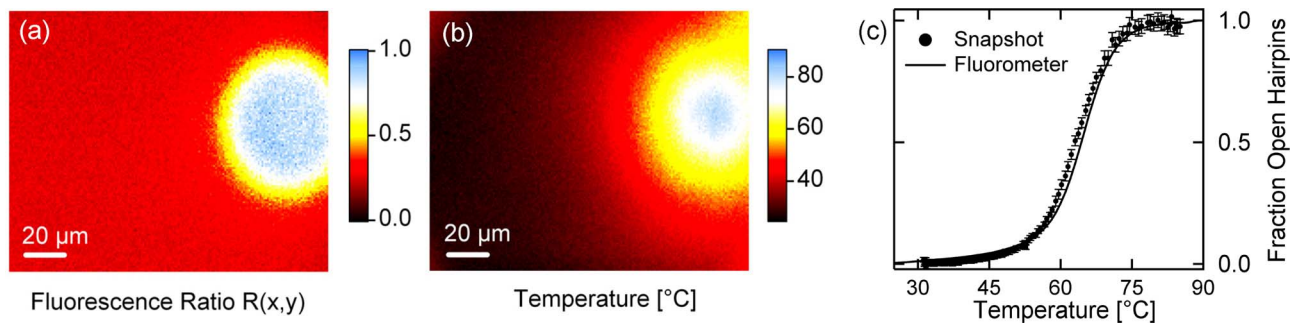
FIG. 2. Melting curve within a 50 ms snapshot: (a) The fluorescence ratio image $R(x,y)$ between heated and unheated conditions for 100nM DNA hairpins. The fluorescence is increased in the heated spot. (b) The temperature $T(x,y)$ is imposed to a 20 μm thin water film by infrared laser illumination and is measured using temperature sensitive fluorescence. (c) The fraction of open hairpins (circles), derived from the radially averaged fluorescence ratio $R(r)$ is plotted against the radially averaged temperature $T(r)$. It coincides well with a melting curve obtained from a 2 h fluorometer measurement (solid line).

The temperature image $T(x,y)$ is measured from a second experiment with the temperature dependent dye tetramethylrhodamine (TAMRA) (Invitrogen). Laser power, chamber geometry, and camera timing are kept fixed. For calibration, the temperature dependent fluorescence signal $F_{TAMRA}(T)$ of TAMRA is measured in a 0.5$\times$ SSC-buffer (75mM NaCl, 7.5mM Na3-citrate, 0.01% TWEEN 20, pH 8.1) with a thermally controlled fluorometer (Fluoromax. 3; Horiba Jobin Yvon GmbH). From $F_{TAMRA}(T)$ we infer $T(F_{TAMRA})$ as shown in Fig. 3(a). With this calibration, we
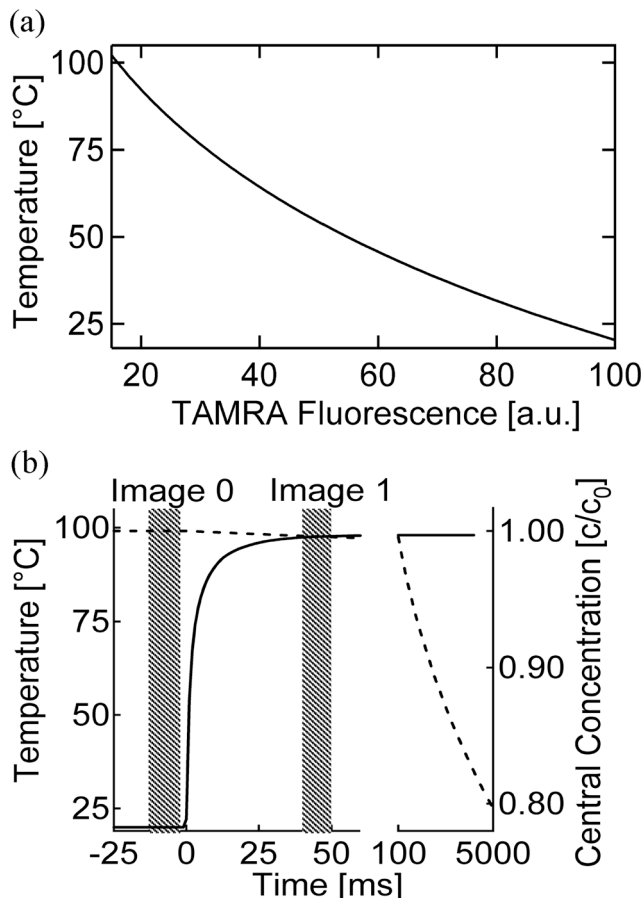

FIG. 3. Temperature and timing: (a) Calibration curve of the temperature dependent dye TAMRA in SSC-buffer used to infer the chamber temperature. (b) Simulations show that a precise synchronisation between laser heating and image exposures is crucial to reach a steady state in temperature (solid line) and not to significantly decrease the molecule concentration in the center of the chamber due to thermophoresis (dotted line).

can transform the TAMRA fluorescence image $F_{TAMRA}(x,y)=I_1(x,y)/I_0(x,y)$ into a temperature image $T(x,y)$. As before, the images I_0 and I_1 are corrected against camera background and bleaching.

The spatial temperature distribution was generated by the light absorption in water. We used a fiber coupled IR laser (Raman fiber laser RLD-5-1455; IPG Photonics Corporation) with a wavelength of 1455 nm and typically applied an output power of 1.2 W. Water absorbs at this wavelength with an attenuation length of 305 μm. The laser beam was moderately focused with a lens of 8 mm focal distance and switched on and off by moving the laser spot into the field of view with galvanometric mirrors. A fluorescence microscope (AxioTech Vario; Zeiss) with an oil immersion objective (40$\times$, 1.3 numerical aperture, Zeiss Fluar) was used. Two 170 μm thick coverslips (12 mm diameter) sandwiched 2 μl aqueous solution and were sealed with nail polish to prevent evaporation. Chamber thickness was 20 μm. The sample was illuminated with a mercury lamp (HXP 120, Leistungselektronik Jena GmbH). A TAMRA fluorescence filter set was used (AHF Tübingen, Germany) and the laser was blocked with OD5 using a glass filter (KG 5, AHF Tübingen, Germany). Imaging was provided with a 12-bit CCD camera (Sensicam QE; PCO AG). The DNA hairpin was purchased from biomers.net with the sequence 5′-Hex-GCA CGC ATC GCT CTT CAT TAG AAC TAT GCG TGC-Dabcyl-3′ and diluted to 100nM in 0.5$\times$ SSC-buffer.

Several artifacts have to be exluded to be able to measure a melting curve in the described setting. We simulated the heat conduction numerically in the axial symmetric geometry of the chamber.[9,10] The temperature relaxes with a time scale which is essentially given by the heat diffusion relaxation time perpendicular to the chamber,

$$\tau = \frac{d^2}{\pi^2}\frac{C\rho}{k}. \tag{1}$$

We find $\tau=0.32$ ms for a thickness of the chamber of $d=20$ μm, the heat capacity of water $C=4200$ J/(kg K), the thermal conductivity of water $k=0.54$ W/(K m), and the density of water $\rho=1000$ kg/m^3. The glass chamber walls conduct the heat comparably to water with $k \approx 0.8$ W/(K m). This results in an effective increase of the thermal thickness d which changes the thermal relaxation time to 2.2 ms, seen in the numerical simulation [Fig. 3(b), solid line]. The time of 40 ms between the two images therefore ensures a steady state temperature distribution. Due to

the low conducting glass walls the temperature distribution along the z direction follows a flat parabolic profile.[10]

The most important condition is that the molecule concentration within a pixel of the chamber has to remain constant between the two images I_0 and I_1. Due to an effect known as thermophoresis,[9–11] molecules drift along a temperature gradient. Thermophoresis is parametrized with a thermophoretic mobility D_T relating the molecule velocity to the thermal gradient ∇T according to $v = -D_T \nabla T$. In the steady state, the molecule concentration at a given temperature difference ΔT is given by $c/c_0 = e^{-S_T \Delta T}$,[12] with the Soret coefficient defined as $S_T = D_T/D$. For the hairpin system, we simulated thermophoresis numerically using $D_T = 1.15 \ \mu\mathrm{m}^2/(\mathrm{s\,K})$ and $D = 115 \ \mu\mathrm{m}^2/\mathrm{s}$,[9,13] and find that the temperature gradients along the chamber result only in a $<1\%$ drop of the central concentration within 50 ms [Fig. 3(b), dashed line]. Similarly, the thermophoresis of TAMRA does not affect the temperature measurement. The maximum velocity of thermal convection is calculated to 1.4 $\mu\mathrm{m/s}$ (Ref. 10) and has no effect within the measurement time window.

Epifluorescence in a 20 $\mu\mathrm{m}$ thin chamber averages the fluorescence of the chromophores across the chamber. We probed for thermal lensing effects by comparing objectives with different numerical apertures and found no significant effect under the given defocused laser spot conditions. The IR laser is blocked after the objective; however, tests using dried films of TAMRA with and without laser illumination show no effects of the laser irradiation on imaging.

The folding and unfolding of a DNA hairpin equilibrates on the microsecond to millisecond time scale.[14] Therefore, we can expect that the melting curve is measured in the kinetic equilibrium. As shown in Fig. 4, we fitted the melting curve with a two state model to extract the standard enthalpy ΔH^0 and entropy ΔS^0 of the reaction according to $\Delta G^0 = -RT \ln(K) = \Delta H^0 - T \Delta S^0$. Standard protocols were used to infer the fraction of closed to open states of the hairpin molecule and thus the equilibrium constant (K) from the melting curve.[2,5] We find $\Delta H^0 = -253$ kJ/mol and $\Delta S^0 = -754$ J/(mol K) and thus a melting temperature of 62 °C. This result comes very close to the calculations of DNA hairpin thermodynamics, predicting $\Delta H^0 = -275$ kJ/mol and $\Delta S^0 = -813$ J/(mol K) and a melting temperature of 65 °C.[15]

We developed a method for the fast measurement of high precision melting curves. Based on an all-optically generated spatial temperature distribution, the method circumvents the slow equilibration time of conventional melting curve analy-
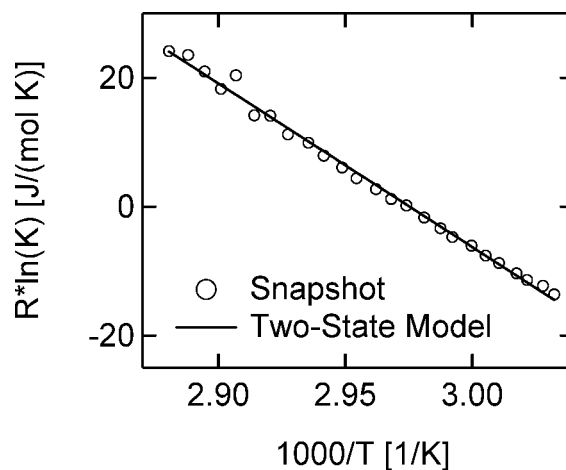

FIG. 4. Thermodynamic analysis: Fitting a two state model to the melting curve data allows one to infer the standard enthalpy and entropy of the reaction.

sis and accelerates the analysis more than 10 000 times from about 10 min down to 50 ms. The detection volume is as low as 2 nl and measurements at 100nM concentration are demonstrated. The method is of particular interest for high throughput screening in biotechnology and fast genotyping in medicine.

[1] J. Marmur and P. Doty, J. Mol. Biol. **5**, 109 (1962).
[2] J. L. Mergny and L. Lacroix, Oligonucleotides **13**, 515 (2003).
[3] M. G. Herrmann, J. D. Durtschi, L. K. Bromley, C. T. Wittwer, and K. V. Voelkerding, Clin. Chem. **52**, 494 (2006).
[4] S. Tyagi and F. R. Kramer, Nat. Biotechnol. **14**, 303 (1996).
[5] G. Bonnet, S. Tyagi, A. Libchaber, and F. R. Kramer, Proc. Natl. Acad. Sci. U.S.A. **96**, 6171 (1999).
[6] J. M. Akey, D. Sosnoski, E. Parra, S. Dios, K. Hiester, B. Su, C. Bonilla, L. Jin, and M. D. Shriver, BioTechniques **30**, 358 (2001).
[7] S. O. Sundberg, C. T. Wittwer, J. Greer, R. J. Pryor, O. Elenitoba-Johnson, and B. K. Gale, Biomed. Microdevices **9**, 159 (2007).
[8] T. Liedl and F. C. Simmel, Anal. Chem. **79**, 5212 (2007).
[9] S. Duhr and D. Braun, Proc. Natl. Acad. Sci. U.S.A. **103**, 19678 (2006).
[10] S. Duhr, S. Arduini, and D. Braun, Eur. Phys. J. E **15**, 277 (2004).
[11] C. Ludwig, SB Akad. Wiss. Wien **20**, 539 (1856).
[12] S. Duhr and D. Braun, Phys. Rev. Lett. **96**, 168301 (2006).
[13] P. Baaske, F. M. Weinert, S. Duhr, K. H. Lemke, M. J. Russell, and D. Braun, Proc. Natl. Acad. Sci. U.S.A. **104**, 9346 (2007).
[14] G. Bonnet, O. Krichevsky, and A. Libchaber, Proc. Natl. Acad. Sci. U.S.A. **95**, 8602 (1998).
[15] M. Zuker, Nucleic Acids Res. **31**, 3406 (2003).